

Computationally efficient framework for probabilistic collapse analysis of structures under extreme actions

Mohammad Mahdi Javidan^a, Hyungoo Kang^a, Daigoro Isobe^b, Jinkoo Kim^{a,*}

^a Department of Civil & Architectural Engineering, Sungkyunkwan University, Suwon, Republic of Korea

^b Division of Engineering Mechanics and Energy, University of Tsukuba, Ibaraki, Japan

ARTICLE INFO

Keywords:

Finite element method
Neural network
Impact load
Reliability
Sensitivity
Fragility

ABSTRACT

Currently there is a growing need for a versatile framework consisting of analytical and surrogate models to ensure both accuracy and computational efficiency of collapse analysis under extreme actions. However training metamodels for highly nonlinear structural responses requires large number of samples to achieve enough accuracy. In this research a method is developed to achieve computational efficiency by implementing the adaptively shifted integration-Gauss technique in conjunction with a core neural network metamodel. The analytical model is validated by experimental data and its accuracy is further evaluated by detailed finite-element analysis. The applicability and efficiency of the provided tool for highly nonlinear analyses are investigated using collapse assessment of a steel framed structure subjected to code-stipulated vehicle impact loads. Thorough probabilistic analyses are carried out including reliability assessment, fragility analysis, and two different sensitivity tests. The analysis results show the superiority and precision of this framework compared to detailed finite-element analysis.

1. Introduction

Undoubtedly there is a growing trend towards probabilistic collapse assessment of structures in recent years [1–3]. Evaluating a structure under such condition needs intensive finite-element (FE) analyses to find collapse probability. The problem becomes worse for fragility and global sensitivity analysis. To overcome this problem, various techniques and soft computing methods have been used such as artificial neural networks (ANN), response surface methods, Kriging, etc. The comparison of these methods for application in seismic fragility analysis has been done recently by Wang et al. [4]. ANN metamodels are universal estimators and their accuracy does not depend on the dimension of the input space compared to polynomial response surface methods [5]. In the latter case, the accuracy is highly dependent on the number of input parameters. Furthermore, response surface methods are based on a specified function in advance while activation functions in ANN metamodels can be adjusted by some coefficients based on inputs and outputs in order to minimize the error. Thus response surfaces might not be able to capture highly nonlinear responses [4]. It has been also shown that nonlinear regression using ANNs has sometimes superiority over Kriging [4]. Based on the aforementioned advantages, ANN has gained a prominent position among optimization techniques [6–8]. However preparing samples for training ANNs using FE analysis is very

costly in terms of computational time, and highly nonlinear problems generally require thousands of samples to achieve adequate approximation using ANN metamodels. On the other hand, simulating the collapse behavior of a structure under one specific scenario needs a detailed analytical model to capture inherent nonlinear and non-monotonic structural responses which in turn is quite time-consuming [9]. In addition to applications to plane frames, trusses, or simple structures [7,8,10,11], neurocomputing has been successfully applied to analysis of large scale structures [12,13]. However collapse simulation under extreme actions is still a matter of debate, especially when a probabilistic analysis is involved. Analyzing structures under such condition may directly result in numerical instability or need time consuming numerical methods for convergence.

In order to partly deal with this problem, the alternate path method (APM) recommended in the design guidelines [14,15] has been employed in many studies to investigate the collapse behavior of different structures [2,16–20]. The prevalent assumption in these studies is based on the speculation that the sudden column removal approach gives conservative results; however this assumption does not hold for every case. For instance, Kang and Kim [21] investigated collapse behavior of moment frames subjected to vehicle collision. The study showed that as a result of large lateral loads during collision, the maximum vertical displacement of the beam-column joint above the impact location is

* Corresponding author.

E-mail addresses: javidan@skku.edu (M.M. Javidan), isobe@kz.tsukuba.ac.jp (D. Isobe), jkim12@skku.edu (J. Kim).

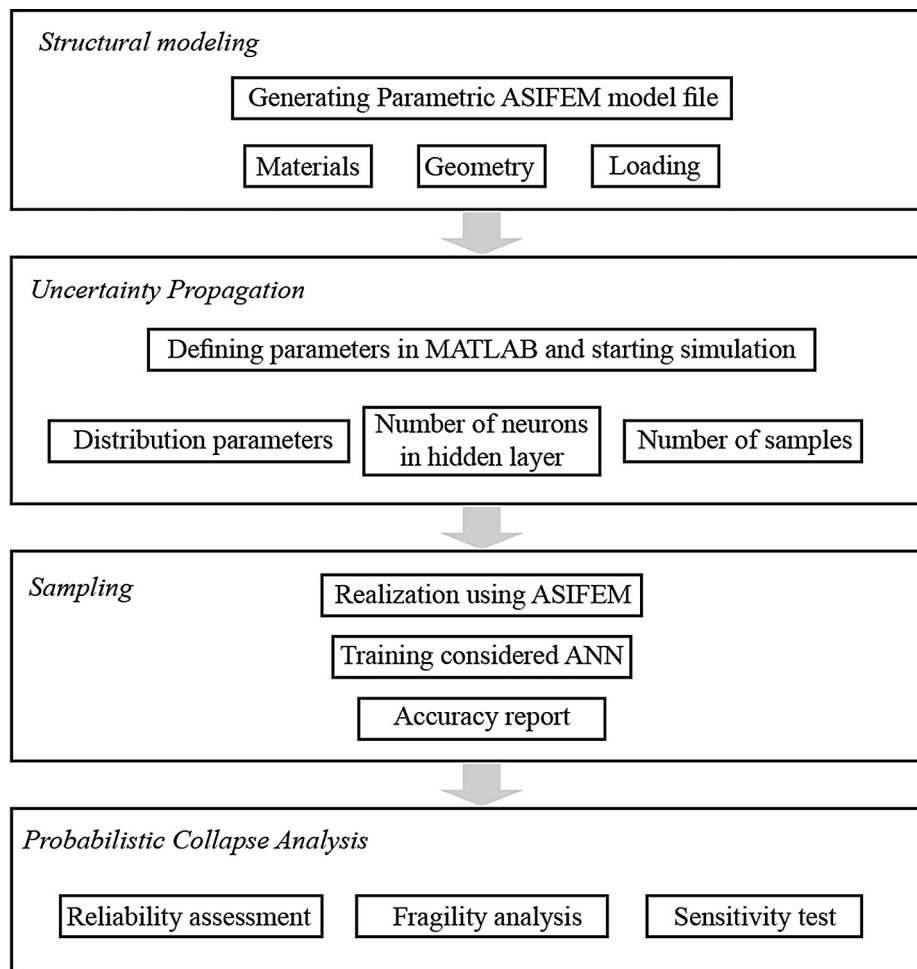


Fig. 1. Representation of the developed framework.

much larger than displacements obtained from APM. Fu also [22] reported that using APM in the collapse assessment of building structures fails to consider large shear actions on column members.

Therefore, a versatile framework including both analytical and surrogate models is required to provide enough accuracy and computational efficiency for collapse assessment under extreme actions. The overall scheme of the framework developed in this study is shown in Fig. 1. A reliable modeling approach called the adaptively shifted integration (ASI)-Gauss technique is utilized to fulfill the requirements for a precise collapse simulation of framed structures under any loading condition. The analytical model is first validated using experimental data, and then the structural modeling procedure is embedded in MATLAB programming [23] to generate the analysis model parametrically. A core ANN metamodel is implemented in the code which is trained by the samples from the parametric model structure. Accordingly uncertainty propagation, assigning ANN parameters, and defining the number of samples for training procedure can be done in the developed framework. The number of samples and ANN parameters can be changed based on the accuracy report to get the adequate approximation. At the next stage, samples from the analysis model are implemented with a proper neural network architecture to conduct further probabilistic analyses at a low computational cost. To show the applicability of the presented method for probabilistic collapse analysis under large deformations, a steel structure subjected to code-stipulated vehicle impact loads is investigated when uncertainties in loading, geometry, and material properties are present.

Most studies about collapse analysis of structures under vehicle impact have assessed the impact behavior of column members, though

the post-collision behavior of the structure at hand is of great interest. For instance, El-Tawil et al. [24] evaluated the behavior of bridge piers under vehicle collision and found that current standard provisions in this field are non-conservative. Sharma et al. [25,26] assessed shear capacity of reinforced concrete columns probabilistically and developed methods for estimating the fragility curves under vehicle collision. Kang and Kim [27] studied effects of different footing connection details on impact behavior of a steel column. Here, a whole structure is investigated using reliability and fragility analysis under vehicle impact loads on a corner column according to the European code [28]. The accuracy of the model structure is further evaluated by comparing its collapse behavior with a detailed FE model. To find the most influential uncertain variables, the tornado diagram analysis (TDA) is carried out and the results are compared with a variance-based global sensitivity test. By taking advantage of the presented framework Monte Carlo simulations (MCSs) are carried out efficiently.

The present research may provide a framework for different types of probabilistic and reliability-based collapse analysis under extreme loads, which is of great interest in practice. Furthermore, the comparison of different sensitivity tests will show the tradeoff between efficiency and accuracy which is helpful for researchers.

2. Computationally efficient analytical model

2.1. ASI-Gauss technique

To get the response of the structure under extreme loads, the ASIFEM code [29] is employed which takes advantage of the ASI-Gauss

technique. This technique provides computational efficiency in problems with highly nonlinear behavior such as collapse analysis. Based on numerous advantages of the ASI-Gauss technique and its flexibility in application to different problems, it has been utilized in a wide variety of structural analyses such as impact loading [30], progressive collapse [31], seismic collapse [32], and demolition [33].

The main idea in the ASI technique is to shift the integration point in the beam element when a plastic section occurs to form a plastic hinge at the exact location. When the plastic hinge is unloaded, the numerical integration point is shifted back to the first position, thus capturing the material-unloading behavior accurately. The relationship between the locations of the numerical integration point and the plastic hinge is obtained using the strain energy approximation of the FE beam model and Rigid Bodies-Spring model (RBSM). This model consists of rigid bars connected with rotational and shear springs, simulating the relative rotational and sliding behavior of the adjacent bars.

In order to increase the solution accuracy in the elastic range, the ASI technique is modified to the ASI-Gauss technique [30]. In this technique, two consecutive element is considered as a subset of a member. The numerical integration points of two consecutive elements are considered in such a way that the stress evaluation points in the elastic range coincide with the Gaussian integration points of the member. The stresses and strains in the elastic range are evaluated at the Gaussian integration points using two-point integration while one-point integration is actually used per element. In this way, the appropriate elasto-plastic behavior of a member can be attained using fewer elements and the rate of solution convergence is improved. Detailed information regarding this technique can be found in Isobe [33].

2.2. Validation for progressive collapse potential

Although ASIFEM has been utilized and validated in different fields, the accuracy of this code for simulating progressive collapse is further validated in this study. For this purpose, the test results of the steel structure with welded unreinforced flange-bolted web (WUF-B) shown in Fig. 2 [34] is compared with the analysis results of ASIFEM. The specimen is a full-scale two-span steel beam from the exterior moment-resisting frame of a building designed for Seismic Design Category C. The unsupported middle stub is monotonically subjected to a downward displacement, simulating column removal. Two diagonal braces are rigidly connected to the top of each column and are attached to the floor. These braces do not participate in resisting the vertical deflection of the beams, but only restrain the ends of the columns to simulate the

Table 1
Mechanical properties of the WUF-B specimen.

Component	f_y (MPa)	f_u (MPa)	ϵ_y	ϵ_u
Beam web	395	500	0.0019	0.189
Beam flange	359	496	0.0017	0.174
Column	352	456	0.0018	0.190

effect of beams and bracing on upper floors. Material properties of the subassemblage are given in Table 1.

The analysis model is established in ASIFEM based on the symmetric condition and the column restraint is modeled as the ideal fixed-end support. In the ASIFEM code, materials are modeled using a perfectly elastic-plastic behavior with bilinear isotropic hardening as the constitutive model. Each material assigned to a section is defined using Young’s modulus, Poisson’s ratio, yield strength, strain hardening modulus, and density. Each section is defined based on the area, torsional coefficient, moment of inertia, and plastic modulus about the weak and strong axis. Since each section is defined using one specific yield strength in ASIFEM, the yield strength of the beam flange is taken for the whole beam section. The Young’s modulus and the strain hardening ratio are also calculated using the reported information. Geometric nonlinearities, i.e. large deformations and strains, are taken into account using the updated Lagrangian formulation. The analysis model for ASIFEM is depicted in Fig. 3(a), and the comparison between the analysis results and the experimental data are presented in Fig. 3(b). As can be seen in Fig. 3(b) the ASIFEM model can simulate the collapse behavior of the subassemblage under large deformations reasonably well.

3. Neural network metamodels

The Monte Carlo simulation (MCS) method can be employed for both reliability and sensitivity analyses by generating a large ensemble of samples and evaluating their structural responses. In spite of its simplicity and robustness, this method is quite costly in terms of computational time. Many methods have been proposed to alleviate the problem, including ANNs which have proved to be an efficient surrogate model for reliability analysis [8,35,36].

ANNs aim at mapping from an input variable space to a response space using a number of simple mathematical models called artificial neurons. Each neuron, as depicted in Fig. 4, consists of the input

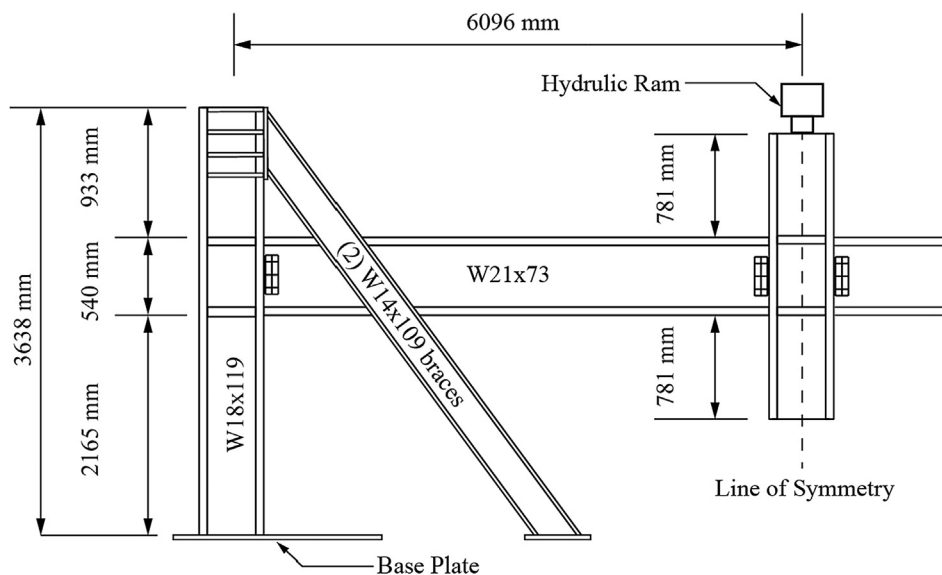


Fig. 2. Details of the test specimen.

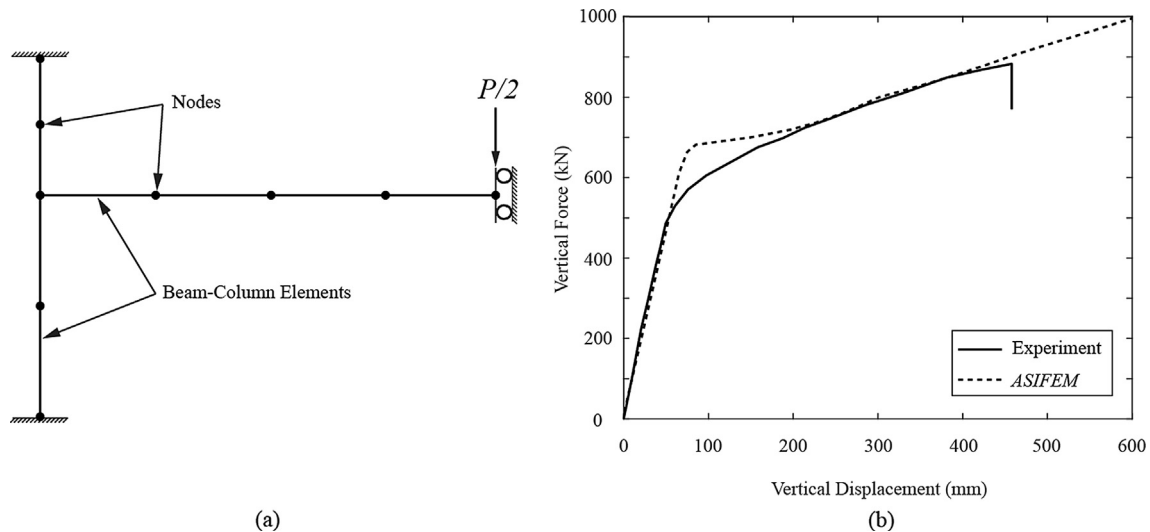


Fig. 3. Validation of ASIFEM: (a) Analysis model; (b) comparison between analysis and experimental results.

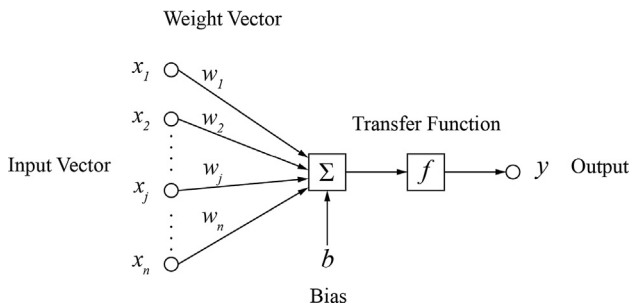


Fig. 4. Artificial neuron.

channels receiving the input vector $[x_i]$, weights $[w_i]$, bias b , transfer function f , and one output channel y . The input signals are multiplied by the weights and summed with the bias as a corrective term. To generate the output y , the summation is input to the transfer function which is usually one of the Linear, Tan-sigmoid, Log-sigmoid, or Step functions. Due to nonlinearity and continuity, the Tan-sigmoid transfer function, i.e. hyperbolic tangent sigmoid, is commonly used in various problems [8,37]. This process with consideration of the Tan-sigmoid function can be expressed as,

$$y = f(w \cdot x + b) \tag{1}$$

$$f(x) = \frac{2}{1 + e^{-2x}} - 1. \tag{2}$$

To make a confident prediction given the input vector, the weights and bias must be well-balanced. Finding these parameters is called training process which can be done using training algorithms and a training set from previous experimental or numerical tests. Linking neurons to each other and arranging them with a proper network architecture leads to a versatile tool called artificial neural networks. One of the most efficient network architectures is the multilayer feed forward network which is able to approximate highly nonlinear functions, if properly trained [36]. In this network there are several layers of neurons and the signals are transmitted from one layer to the next layer in one direction. The neurons are arranged in parallel at each layer while linked to all neurons of the next layer. Therefore the number of neurons in the input and output layer is equal to the number of input and output signals. Since the efficiency of multilayer feed forward networks in uncertainty and reliability analysis has already been demonstrated [7,8], it is therefore chosen for prediction of the structural response in this study.

Uncertainty propagation, sampling, and training the core ANN in the application are done automatically using *MATLAB* programming, and for each realization the structural response is obtained by calling the *ASIFEM* code from *MATLAB*. Different training algorithms and the number of layers and neurons are evaluated to find the most efficient performance for collapse analysis. By trial and error, the Levenberg-Marquardt training algorithm is selected, and ANNs with the Tan-sigmoid transfer function and one hidden layer seemed to be quite applicable [8]. The number of neurons in the hidden layer is defined by the user. As previously noted by Mitropoulou and Papadrakakis [13], training ANNs within a range of input parameters and using it for extrapolating could be problematic. Hence in the implemented framework, uncertainty parameters are sampled uniformly all over their range using the Latin-hypercube sampling (LHS) technique [38], thus compelling ANNs to interpolate between the values. It should be mentioned that, these samples are for training the ANNs, and when the metamodels are ready the probabilistic analyses are done using the specified distributions. The reason for training with uniformly sampled parameters is that the ANN trained with specific distributions might lead to a biased estimator, and it might not be properly applicable to other studies like fragility analysis. Certainly, small number of samples corresponding to low probability cases exist and this could result in some error afterwards. In order to eliminate spurious correlation and have evenly distributed samples with good space-filling properties, all samples are generated five times iteratively and the minimum distance between them is maximized [39,40]. The data for training ANNs are standardized and normalized automatically by *MATLAB* for feed forward networks. The accuracy report is provided by using 30% of the samples for test and validation. Therefore number of neurons and samples can be changed to get desired approximation.

4. Case study structure

To show the applicability, accuracy, and efficiency of the established framework, a steel building structure is analyzed under vehicle impact loads on the corner column. In order to get insight into the accuracy of the analysis model under applied impact loads, structural responses of the model in *ASIFEM* are compared to those of a detailed FE model.

4.1. Structural representation

The model structure used in the analysis is a steel moment resisting frame with three bays and three stories designed for dead and live loads

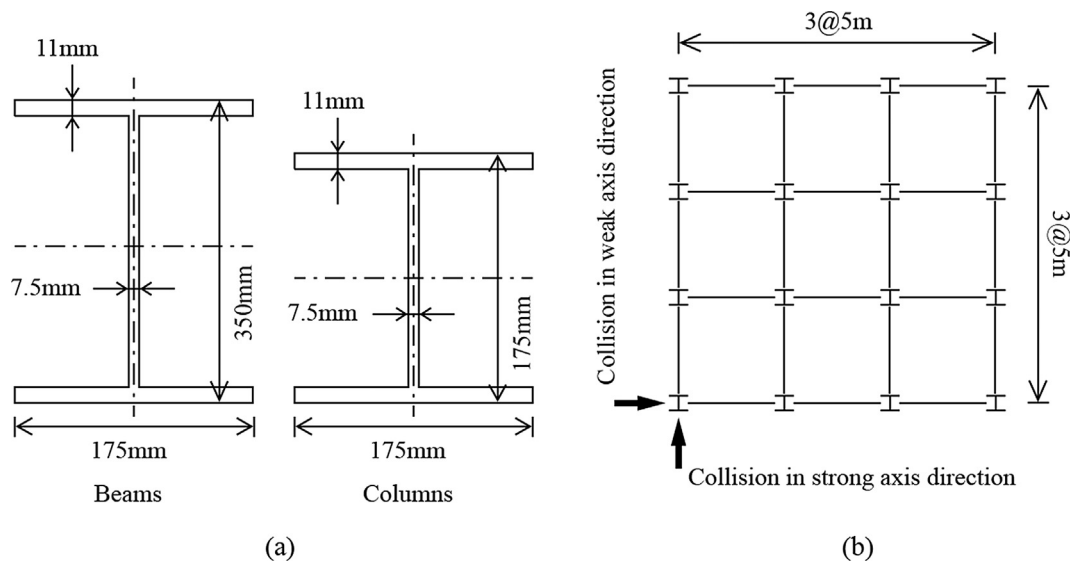


Fig. 5. Structural representation: (a) cross-sectional dimensions; (b) plan layout and collision scenarios.

of 5 kN/m² and 3 kN/m², respectively. All structural members are H-shaped sections with a Young’s modulus of 2×10^5 MPa. The yield strength of beams and columns are respectively 330 MPa and 370 MPa. The cross-sectional dimensions of beams and columns are shown in Fig. 5(a). The first story height is 5 m and the heights of the other two stories are 4 m. As structures are generally more vulnerable to accidental actions on corner columns [16,21], vehicle collision scenarios with the weak and strong axis directions of the corner column are considered. The plan layout of the model structure and the collision scenarios are presented in Fig. 5(b).

4.2. Uncertainty propagation

The properties of the structure presented above are nominal values while in this section uncertainties in the loading, geometry, and materials are described. A total of nineteen uncertainty parameters are considered in this study which are shown in Table 2. The abbreviations provided in Table 2 are used to present the results of the study. The dead load *DL* is normally distributed with a 5% increase over the mean value [41]. The live load *LL* can be divided into the sustained load and the intermittent load [42]. The sustained load is also called ‘arbitrary-

point-in-time live load’ [41] because this load presents the average load during a particular occupancy while the intermittent load or the extraordinary load is related to a rather short duration such as renovation, gatherings, etc. As the vehicle collision is also an arbitrary-point-in-time incident, only the uncertainty in the sustained load is considered. The load combination of $DL + 0.25LL$ is applied according to [15].

The variations of the material properties are represented by a multivariate lognormal distribution according to [42]. The variabilities in the yield strength and Young’s modulus are considered. The mean values for the elastic moduli are considered to be equal to the specified nominal values. The mean yield strength can be calculated as

$$f_y = f_{ysp} \cdot \alpha \cdot \exp(-u \cdot v) - C \tag{3}$$

where f_{ysp} is the specified nominal yield strength; α is the spatial position factor accounting for the subtle difference in the yield strength of webs of hot rolled sections with a factor of 1.05; u is a factor showing the discrepancy between the nominal and mean value, ranging between -1.5 to -2.0 for sections produced with European standards (EN standards) [42]; v is the variability or *c. o. v* equal to 0.07; and C is the yield strength reduction constant for which the value of 20 MPa is recommended. In this study α and u are assumed to be 1.0 and -1.5 ,

Table 2
List of uncertainty parameters.

Category	Parameter	Mean	c. o. v or σ	Distribution	References
Gravity loads	Dead load <i>DL</i>	5.25 kN/m ²	0.10	Normal	[41]
	Live load <i>LL_{apt}</i> ^a	0.575 kN/m ²	0.4	Gamma	
Steel properties	Yield strength of beams f_{yb}	346 MPa	0.07	Lognormal	[42]
	Yield strength of columns f_{yc}	391 MPa	0.07		
	Elasticity modulus for beams E_b	Nominal value	0.03		
	Elasticity modulus for beams E_c	Nominal value	0.03		
Cross-sectional dimensions for both beams and columns	Outside height t_1	Nominal value	0.05	Normal	[41,42]
	Flange width t_2				
	Flange thickness t_f				
	Web thickness t_w				
Construction tolerances	Beam length L	Nominal value	30.4 mm	Normal	[42,43]
	First story column height H				
Impact load	Vehicle stiffness k	300 kN/m	60 kN/m	Lognormal	[28,42]
	Vehicle mass m	20,000 kg	12,000 kg	Normal	
	Vehicle velocity V	16 km/h	3.2 km/h	Lognormal	

^a Arbitrary-point-in-time live load.

respectively.

It is recommended that the normal distribution can satisfactorily represent geometrical member dimensions [42]. For sectional dimensions, the nominal handbook properties can be taken as the mean value with a $c. v$ of 0.05 for hot-rolled sections [41]. The European Standard [43] specifies that the constructional tolerance on the length of H-sections is ± 50 mm. Hence, it is assumed that the length of a member is normally distributed and the standard deviation is calculated such that 90% of values fall within the stipulated tolerance.

Dynamic vehicle impact loading is based on the European Standard for accidental actions [28]. This formula uses the ‘rigid structure’ assumption while the vehicle is considered as an elastic system. Hence, the maximum interaction force and the impact time can be obtained as

$$F = V\sqrt{km} \quad (4)$$

$$F\Delta t = mV \text{ or } \Delta t = \sqrt{m/k} \quad (5)$$

where V , k , m are respectively the velocity, equivalent elastic stiffness, and mass of the vehicle. In Eurocode an automobile collision impact force is represented by a rectangular pulse. In this study the vehicle is assumed to be a truck and therefore according to [28] the mass in the formula is normally distributed with a mean value of 20,000 kg and a standard deviation of 12,000 kg. To prevent negative mass during sampling, a truncated probability distribution is utilized. The velocity is assumed to be a lognormal variable with a mean and a standard deviation of 16 km/h and 3.2 km/h, respectively. The stiffness is considered as a deterministic parameter in the European Standard with a mean of 300 kN/m, while it is a lognormal variable in the probabilistic model code [42] with a standard deviation of 60 kN/m. In order to incorporate the variability of the stiffness parameter, the vehicle stiffness is also considered as an uncertainty source, following the probabilistic model code. The spatial variation of uncertainty parameters is not considered and it is assumed that all the parameters are spatially correlated in the whole structure.

4.3. Accuracy of the analysis model under impact loads

To validate the accuracy of *ASIFEM* to simulate the overall behavior of structures under impact loads, the case study structure is also modeled in *LS-DYNA* [44] which is a general purpose FE code. The center of the corner column in the detailed model is subjected to an impactor as shown in Fig. 6. The properties of the impactor used in the analysis is given in Table 3. The impact forces obtained from *LS-DYNA* are simplified as rectangular forces as recommended in the European Standard and then are applied to the *ASIFEM* model for efficient analysis and comparison.

The structure is modeled in *LS-DYNA* using solid elements, as shown in Fig. 6(b), with an elastoplastic material called `MAT_PIECEWISE_LINEAR_PLASTICITY`, and the contact is defined using the `CONTACT_AUTOMATIC_SURFACE_TO_SURFACE` keyword. The impactor used to generate the impact force is modeled using the `MAT_ELASTIC` material. The dead and live loads are distributed to the beams according to the tributary area. On the other hand, a simplified model is established in *ASIFEM* under the same condition of the detailed model (Fig. 6(d)). For the impact analysis the simplified model utilized the consistent mass matrix formulation with the aim of improving computational accuracy and the Newmark- β method with an incremental time step of 1 ms with 2% damping ratio.

Fig. 7 shows the time histories of the impact loads generated by the impactor in *LS-DYNA*, which are simplified into rectangular impulses to be used in *ASIFEM*. The simplification is made in such a way that the rectangular impulses and the time history of the impact loads have the same maximum forces and total impulses. The vertical displacements of the beam-column joint above the corner column are compared in Fig. 8. Although there are some discrepancies, there is a reasonable agreement between the results. The outcomes are quite satisfactory considering the

fact that *LS-DYNA* analysis takes almost 112 h using a PC with the Intel® Core i7-7700k processor whereas it takes around 20 s in *ASIFEM*. Although an adaptive mesh could be used to reduce the computational cost of *LS-DYNA* analysis, the computational efficiency of the *ASIFEM* is incomparable when samples in the order of 20,000 are needed. Thus *ASIFEM* is used in the provided framework for sampling and realizations at the first stage, then metamodels are trained with these samples in order to drastically reduce the computational time.

For further analyses, two ANNs corresponding to two collision scenarios along the weak and strong axis of the corner column are considered. The maximum beam rotation in the damaged bay in one second after impact is employed as a measure for the structural response and output of the ANNs for post-collision evaluation. Six training sets with different numbers of samples ranging from 500 to 20,000 are considered for each scenario. The number of neurons in the hidden layer is set to be 20. In the following section, it is shown that these assumptions give adequate accuracy for the problem at hand.

5. Reliability analysis

The reliability analysis of the model structure is conducted with 20,000 realizations. The structural response for each realization is retrieved by both the conventional FE analysis using *ASIFEM* and ANNs trained with different number of samples. The goodness of fit of the ANNs as surrogate models is evaluated and the failure probabilities from both approaches are also compared. The limit state function $g(X)$ for the reliability analysis is defined based on the rotational demand on beams in the damaged bay where X is the vector of random variables for each realization. Their corresponding limit states are defined according to [45] as shown in Table 4. These limit states and failure criteria are related to four damage levels of steel structures subjected to extreme loads which correspond to the light, moderate, and severe damage states.

The failure state is reached when $g(X) \leq 0$, and by using MCS the failure probability is estimated as,

$$P_f = \frac{1}{N} \sum_{i=1}^N I(X_i) \quad (6)$$

where N is the number of realizations equal to 20,000 in this part and I is the failure indicator expressed by,

$$I(X) = \begin{cases} 1 & g(X) \leq 0 \\ 0 & g(X) > 0 \end{cases} \quad (7)$$

The results of the FE-based reliability analysis are compared with the ANN-based ones in Tables 5 and 6 for the two collision scenarios. The required time is considered as the computational cost which also includes the time for sampling and training the ANNs. The goodness of prediction for the 20,000 samples is quantified using the mean absolute error *MAE*, mean squared error *MSE*, and coefficient of determination R^2 . In the next columns, the failure probabilities for three limit states are also shown. It can be seen that the *MAEs* are much smaller than the range between the limit states and as a result the failure probabilities could be approximated reasonably. R^2 and *MSE* are sensitive to outliers but these statistics also show a close prediction. The statistics and comparison between the failure probabilities show that the ANNs trained with more than 5000 samples can predict the structural behavior of both scenarios with a sufficient accuracy. Although ANNs trained with larger sample sets are more accurate, the improvement in precision afterward is not significant compared to the number of samples. By investigating the failure probabilities of the ANN-based MCS and FE-based MCS, it can be inferred that errors are mostly related to collapse extents. This is due to the high nonlinearity and non-monotonicity of the structural response in extensive collapses.

Fig. 9 compares the 20,000 maximum rotational demands on beams obtained from FE analysis with the values predicted by the ANNs

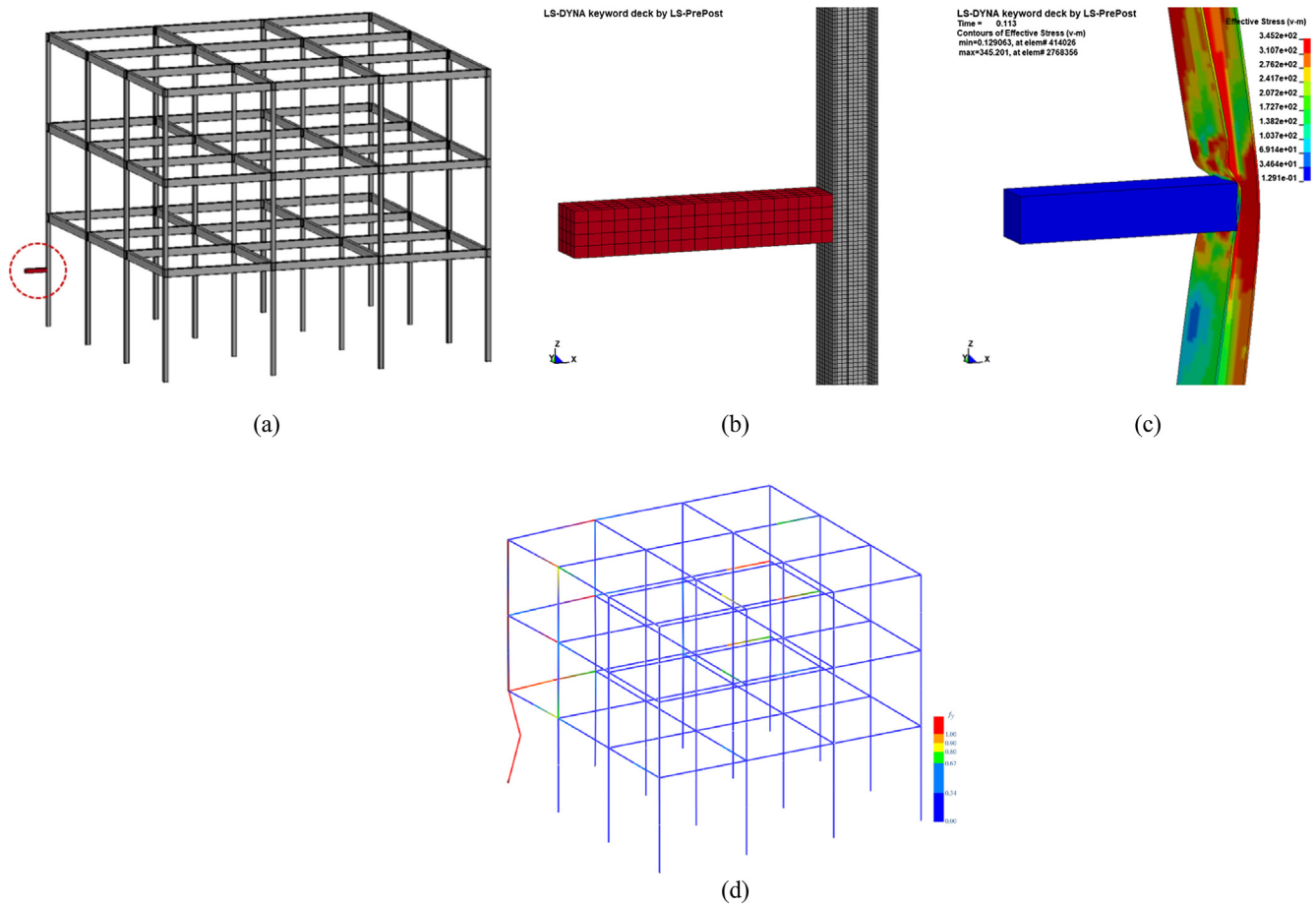


Fig. 6. Configuration of the analysis model subjected to an impact on the corner column: (a) location of the impactor; (b) modeling of the impactor; (c) stress distribution; (d) ASIFEM model.

Table 3
Properties of the impactor used in the impact analysis.

Mass	Velocity	Size	Young's modulus	Stiffness EA/L
7962 kg	20 km/h	175 mm × 175 mm × 1000 mm	10 MPa	306 kN/m

trained with 10,000 samples. The aforementioned fact can be seen in Fig. 9(a) and (b) where the data are more scattered at large deformations, especially for the weak axis scenario which is more critical. The error histograms in Fig. 9(c) and (d) show that the ANNs trained by 10,000 samples produce quite accurate results, and based on the results and the computational costs they are employed for further analyses. Although the ANNs are trained with uniformly distributed samples all over the input and output space, they can practically estimate the failure probability for specific distributions defined for the structure. This means that they can estimate the structural response for any specific realization. The goodness of fit also ensures this ability of the ANNs.

The discrepancies between the presented failure probabilities are partly attributable to the MCS estimation with a small number of samples. According to Shooman [46], the accuracy of a failure probability obtained using MCS can be approximated by the coefficient of variation *c. o. v* as,

$$c. o. v = \sqrt{\frac{1 - P_f}{P_f n_{MCS}}} \quad (8)$$

where P_f is the failure probability and n_{MCS} is the corresponding

number of samples. The minimum failure probability for the case study structure is in the order of 3.4% and is related to the impact along the strong axis direction. To find the failure probability with a *c. o. v* around 1%, approximately 3×10^5 samples are needed. The results for reliability assessment considering the required accuracy and number of samples are shown in Table 7. The reliability indices are calculated using the first-order approximation as follows,

$$\beta = -\Phi^{-1}(P_f) \quad (9)$$

where Φ^{-1} is the inverse cumulative distribution function of the standard normal distribution.

The reliability analysis shows that the model structure is highly prone to collapse under vehicle impact loads on the corner column, especially along the weak axis direction. The failure probability indicates the probability of exceeding a certain damage state. The results show that the probability for severe damage is lower than that of the light damage state. This implies that expecting at least light damage after the collision is more probable. As the reliability indices are proportional to the inverse cumulative distribution function of the failure probability, the reliability indices for the severe damage state is higher compared to that of the light damage state. The recommended minimum reliability index for common structures is $\beta = 3.8$ according to Eurocode [47] which corresponds to $P_f = 7.23 \times 10^{-5}$. Important structures and facilities suffering from this sort of vulnerability can be retrofitted in accordance with the occupancy and risk level. Another decisive factor in making provisions could be based on sensitivity analysis. To have realizations falling in a desirable output range and control the output uncertainties, sensitivity analysis is an invaluable tool which is addressed in the next section. Finally, it is observed that

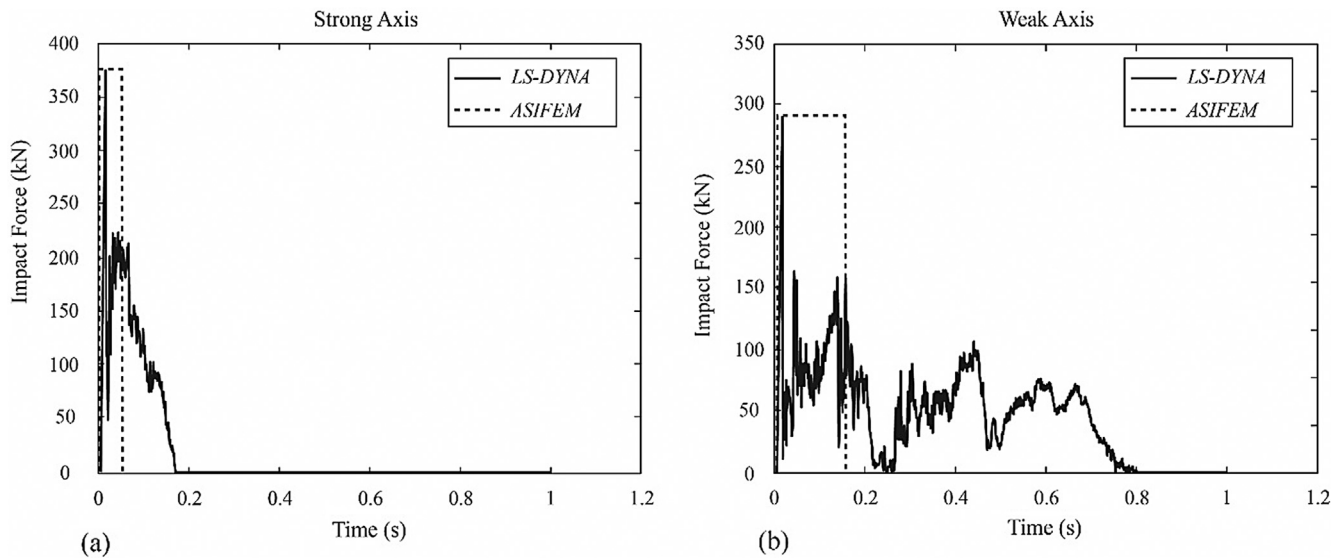


Fig. 7. Time histories of impact loads obtained from LS-DYNA and their simplifications for ASIFEM: (a) strong axis direction scenario; (b) weak axis direction scenario.

there is no much difference between severe damage probabilities along both directions, but this difference is completely tangible for the light damage state.

6. Sensitivity analysis

6.1. Tornado diagram analysis

Sensitivity analysis is usually performed to identify influential factors and their relative importance in a system. In order to simplify a modeling approach or reduce output uncertainties in reliability analysis, the results from sensitivity tests are of paramount importance. Based on a problem at hand and the corresponding setting, different sensitivity tests can be applied. One of the commonly used methods is the tornado diagram analysis (TDA) owing to its simplicity [48]. In this method, it is tried to ascertain the sensitivity of the output to uncertain parameters by varying each parameter between upper and lower bounds while keeping other parameters constant at a base value. The difference between the output values for each parameter is called swing, and it is depicted in descending order using a bar chart named

Table 4

Failure criteria for steel structures under extreme loads.

Element	Failure type	Damage		
		Light (rad)	Moderate (rad)	Severe (rad)
Beams	Bending	0.05	0.12	0.25

tornado diagram. In the present research, the mean value is considered as the base value, and the two bounds for each variable are determined to be twice the standard deviation below and above the mean, except the vehicle mass for which the lower bound is considered to be zero to prevent the negative value for mass. The results of TDA for the two collision scenarios are shown in Fig. 10. The bars are arranged in accordance with FE-based rotational demands, and the ANN-based outcomes are demonstrated correspondingly using solid lines. The mean rotational demand is denoted by a vertical thick line.

It is seen that variations in the vehicle properties are the most influential factors in vehicle impact loading. Overall, the yield strength,

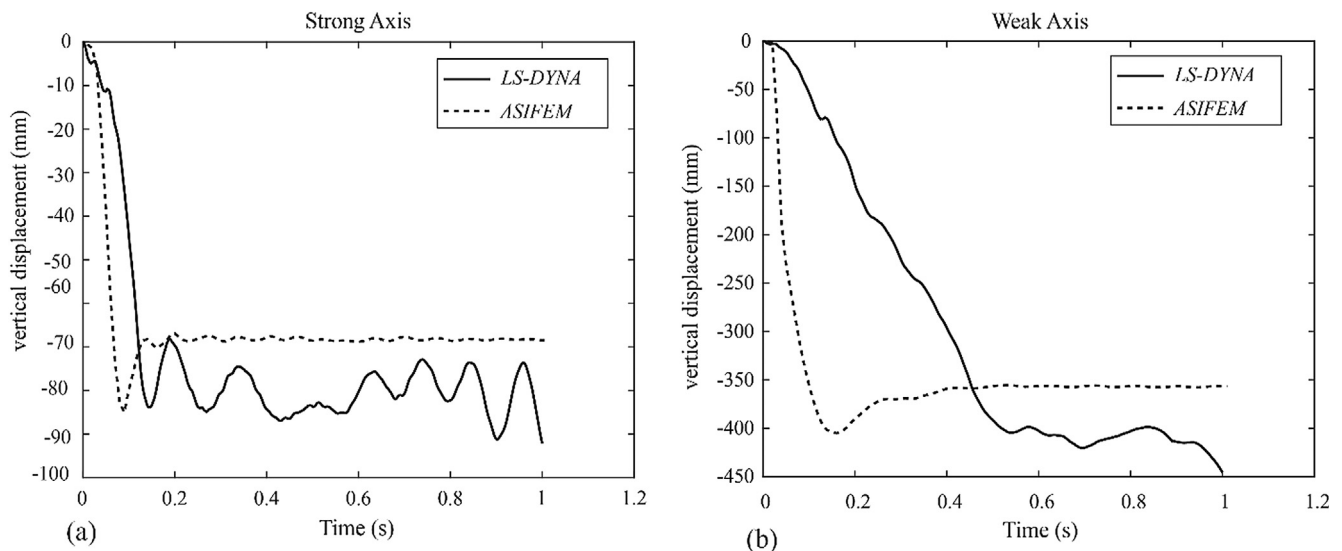


Fig. 8. Vertical displacements at beam-column joint obtained from LS-DYNA and ASIFEM: (a) strong axis direction scenario; (b) weak axis direction scenario.

Table 5
Accuracy of the ANNs for reliability analysis under collision in the strong axis direction.

Method - sample set	Computation time (s)	Goodness of fit			Failure probability		
		MAE	MSE	R ²	Light	Moderate	Severe
					P _f	P _f	P _f
FE - 20,000	385, 882	–	–	–	0.299	0.145	0.034
ANN - 500	10, 949	0.013	5.04 × 10 ⁻⁴	0.907	0.278	0.103	0.025
ANN - 1000	20, 743	0.008	2.06 × 10 ⁻⁴	0.962	0.277	0.124	0.029
ANN - 2000	39, 186	0.006	1.44 × 10 ⁻⁴	0.973	0.300	0.137	0.027
ANN - 5000	93, 827	0.006	1.34 × 10 ⁻⁴	0.975	0.309	0.163	0.039
ANN - 10,000	187, 936	0.005	9.70 × 10 ⁻⁵	0.982	0.311	0.157	0.039
ANN - 20,000	385, 370	0.004	6.11 × 10 ⁻⁵	0.988	0.302	0.145	0.033

flange thickness, flange width, and height of beam-column sections are the next important parameters while variations in the web thickness and elasticity modulus of sections seem insignificant. Uncertainties in geometrical properties and gravity loads do not have considerable influence on the outcomes, especially the live load which has minute effects. Although there are some discrepancies in the FE-based and ANN-based results, the metamodels shows reasonable accuracy. In most cases both methods produce consistent results, which shows that the ANNs can be used as surrogate models for further analysis.

6.2. Global sensitivity analysis

To study the effects of the input parameters in depth and take advantage of the ANNs, a variance-based form of sensitivity analysis is carried out and the results are compared with the TDA. The variance-based sensitivity test, or sometimes called Sobol’s sensitivity analysis, aims to quantify the influence of input parameters on the output variance of a system [49]. The turning point of this method can be found in the work of Sobol [50,51], and it is further refined by Saltelli et al. [49,52]. This method has been widely used in studies on stability of structures with initial imperfections by Kala [53–55]. Arwade et al. [56] also used global sensitivity for structural systems and investigated the effects of input distributions and possible approximation of the response function. A brief description of the global sensitivity analysis is outlined in the following.

Given Y as the scalar output and function of (x_1, x_2, \dots, x_k) , the main contribution of the i th input parameter alone to the total output variance $V(Y)$ is called the first-order index and can be obtained using the

Table 6
Accuracy of the ANNs for reliability analysis under collision in the weak axis direction.

Method - sample set	Computational time (s)	Goodness of fit			Failure probability		
		MAE	MSE	R ²	Light	Moderate	Severe
					P _f	P _f	P _f
FE - 20,000	399, 005	–	–	–	0.639	0.353	0.082
ANN - 500	11, 276	0.025	1.2 × 10 ⁻³	0.853	0.551	0.246	0.055
ANN - 1000	20, 876	0.021	9.00 × 10 ⁻⁴	0.891	0.587	0.267	0.057
ANN - 2000	38, 948	0.014	4.69 × 10 ⁻⁴	0.943	0.622	0.314	0.072
ANN - 5000	94, 919	0.011	3.50 × 10 ⁻⁴	0.957	0.618	0.337	0.088
ANN - 10,000	187, 259	0.011	3.15 × 10 ⁻⁴	0.962	0.629	0.331	0.074
ANN - 20,000	373, 397	0.010	2.87 × 10 ⁻⁴	0.965	0.645	0.339	0.076

conditioned variance as,

$$S_i = \frac{V(E(Y|x_i))}{V(Y)} \tag{10}$$

This indicates that the variance is calculated while varying solely x_i and averaging the output for all possible variations of other input parameters for each fixed x_i . Hence, the influence of varying one parameter can be found and the effects of other parameters are eliminated by averaging over their variations. The sum of the first-order indices $\sum S_i$ is equal to unity for additive models in which there is no interaction between variables. The interaction between x_i and x_j can be stated as,

$$S_{ij} = \frac{V(E(Y|x_i, x_j))}{V(Y)} - S_i - S_j \tag{11}$$

However, obtaining all interactions for a function with k variables needs $2^k - 1$ terms which is impossible in high-dimensional spaces. Therefore another measure called the total effect is employed, which can be determined by:

$$S_{Ti} = 1 - \frac{V(E(Y|x_{-i}))}{V(Y)} \tag{12}$$

where x_{-i} denotes the inner expectation which is conditioned on all variables except x_i . Thus the term $V(E(Y|x_{-i}))$ includes all sources of variation except the i th variable, and by subtracting it from the total variance, the total effect of the considered variable can be calculated. The first-order index along with the total effects can practically show the overall characterization of a model [57]. Further information on global sensitivity analysis can be found in [49].

In the present research, the first-order sensitivity indices and total effects are approximated using MCS and the estimators suggested by Saltelli et al. [49] with a total cost of $N(k + 2)$ runs. The proper number of samples N for the convergence is ensured by conducting the analysis with 100 different sets of N samples and finding the 95% confidence interval (CI) for each N . The sum of the first-order indices for the two scenarios is depicted against the number of samples in Fig. 11. It can be seen as the number of samples increases the CI becomes narrower, the sum of the first-order sensitivity indices converges, and the error of MCS decreases. Based on the observations 50,000 samples are considered with the aim of providing a reasonable accuracy and the results of global sensitivity analysis are reported for this case.

The results from global sensitivity analysis are shown in Fig. 12 and it is seen that they are almost consistent with TDA, though there are some differences in the order of sensitive parameters. These outcomes show the influence of each parameter on the output variance which is different from the viewpoint of TDA. However, based on the results from global sensitivity analysis, it can be concluded that TDA can be used as a quite effective and simple sensitivity test. The major factors in the output response are attributed to the vehicle properties. Sectional properties except the web thickness and elasticity modulus come next

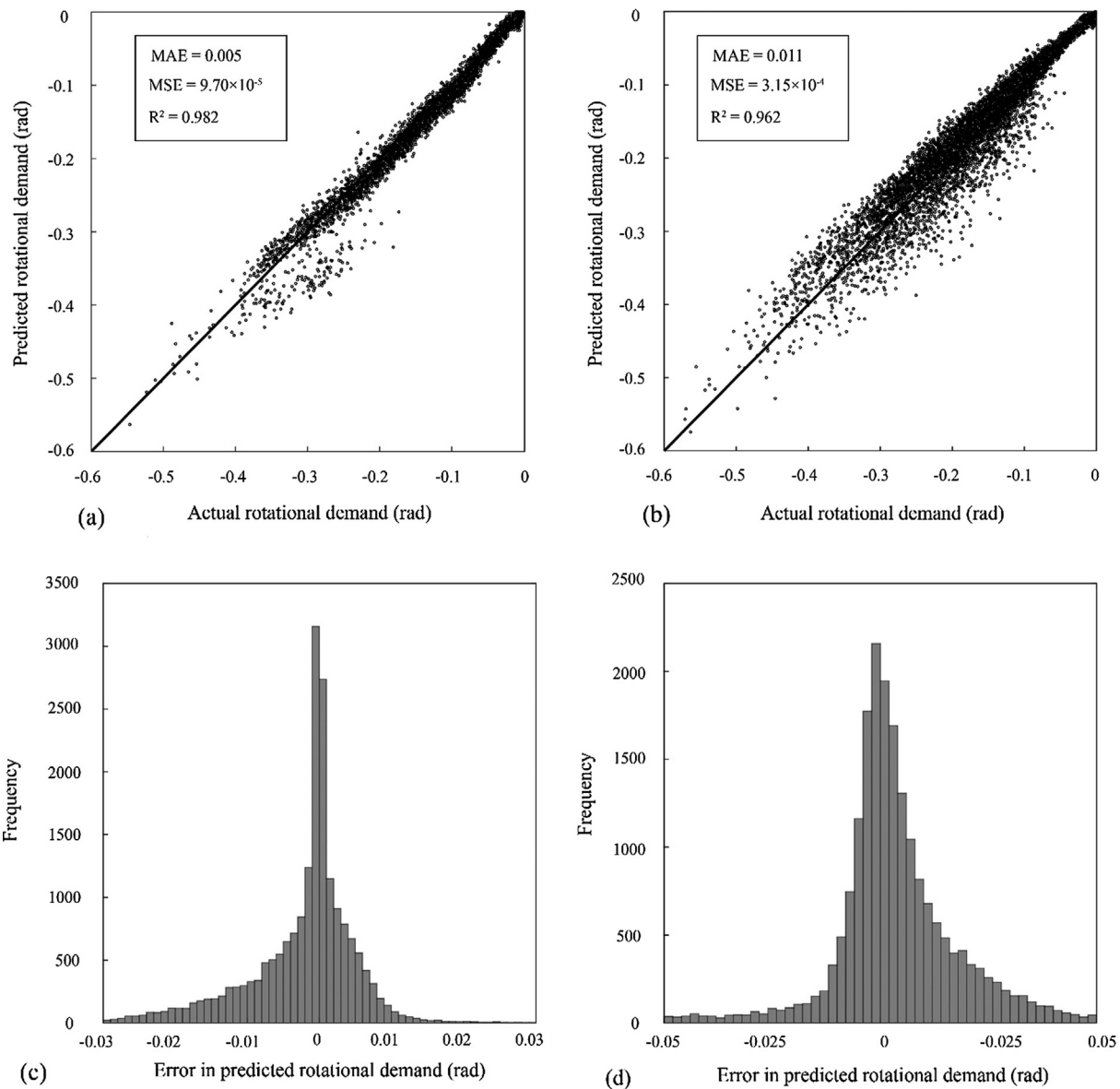


Fig. 9. Comparison of the maximum rotational demands on beams obtained from the FE analysis and the ANNs: (a) strong axis direction scenario; (b) weak axis direction scenario; (c) error histogram for strong axis direction scenario; (d) error histogram for weak axis direction scenario.

Table 7
Results of reliability analysis.

Collision scenario	Limit states								
	Light			Moderate			Severe		
	P_f	β	c. o. v	P_f	β	c. o. v	P_f	β	c. o. v
Strong axis direction	0.314	0.486	0.003	0.159	0.998	0.004	0.041	1.734	0.009
Weak axis direction	0.628	0.327	0.001	0.332	0.435	0.003	0.076	1.431	0.006

like the TDA results. It can be inferred from both sensitivity tests that the flange thickness and yield strength of the corner column is more influential under impact load in the strong axis direction whereas the height and yield strength of the beam have key roles in the other direction. This stems from the fact that the corner column is more vulnerable to impact loads in the weak axis direction and its sectional properties do not contribute substantially to the collapse prevention.

Hence, the beams must span the damaged parts. The superiority of global sensitivity analysis can be found when it comes to interaction effects. The difference between the total effects and the first-order sensitivities show the interaction between parameters and high-order sensitivities. According to the results, interactions other than those between loading parameters do not have much influence on the output variance. Other parameters have therefore negligible effects and one could get the impression that they seem rather insignificant in global sensitivity analysis compared with the results of TDA. It demonstrates the ability of this analysis to quantify the impact of each parameter precisely. Thus, it is worthwhile to mention that considering uncertainties in loading is quite sufficient for probabilistic investigation of structures subjected to vehicle collision. Finally the sensitivity analysis shows that controlling the vehicle velocity, for example by means of security bollards or a proper standoff distance, seems to be the best way of collapse prevention under vehicle collision.

7. Fragility analysis

To elucidate the overall collapse behavior of the structure, fragility

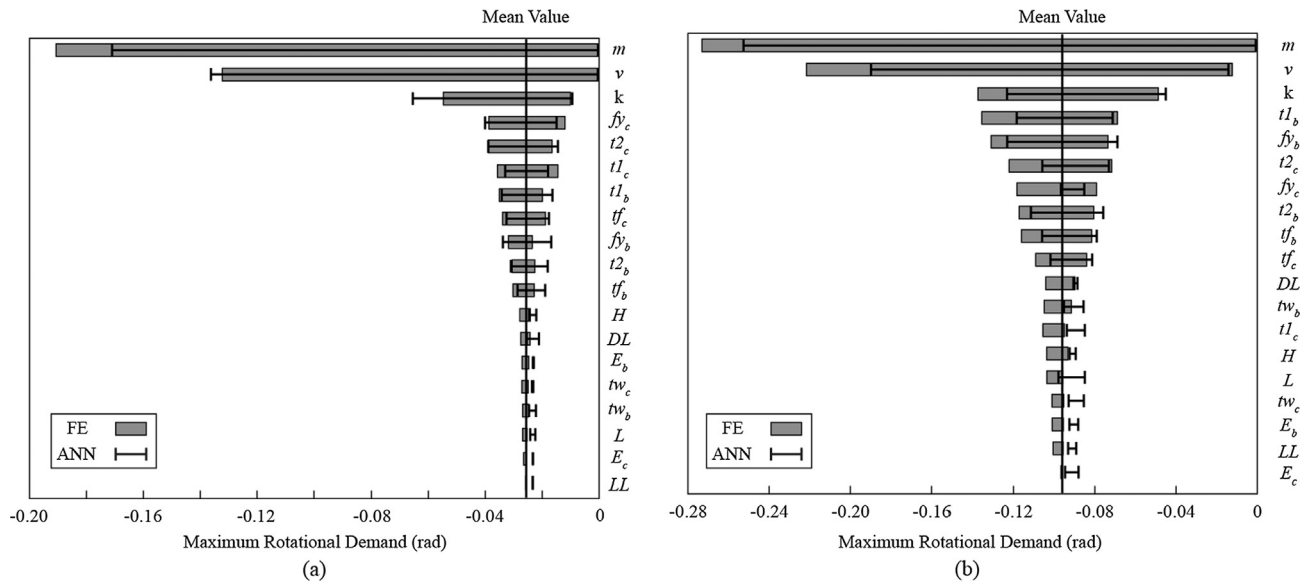


Fig. 10. Tornado diagrams: (a) loading in the strong axis direction; (b) loading in the weak axis direction.

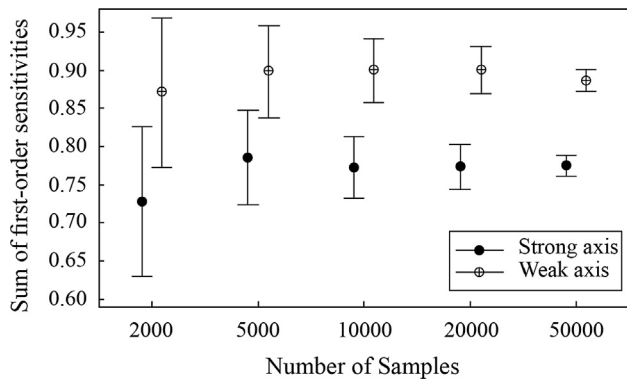


Fig. 11. Convergence of sum of first-order sensitivity indices and its 95% CIs.

analysis is a handy tool and can be done very easily using the developed framework. The fragility function $F_d(x)$ herein gives the conditional probability that the damage measure DM exceeds the limit state d , given x as the intensity measure IM ,

$$F_d(x) = P(DM \geq d | IM = x). \tag{13}$$

The maximum rotational demand on the beams in the damaged bay is considered as the damage measure and the limit states are as mentioned before. Fragility curves have been customarily explained as a function of gravity loads for progressive collapse assessment, even though gravity loads on structures do not vary significantly [2,3,58]. This is because the only suitable parameter for the intensity measure could be the gravity loads when using the threat-independent approach and considering sudden column removal. Instead, the vehicle velocity in the loading formula is considered as the intensity measure in this study. The failure probabilities corresponding to vehicle velocities are

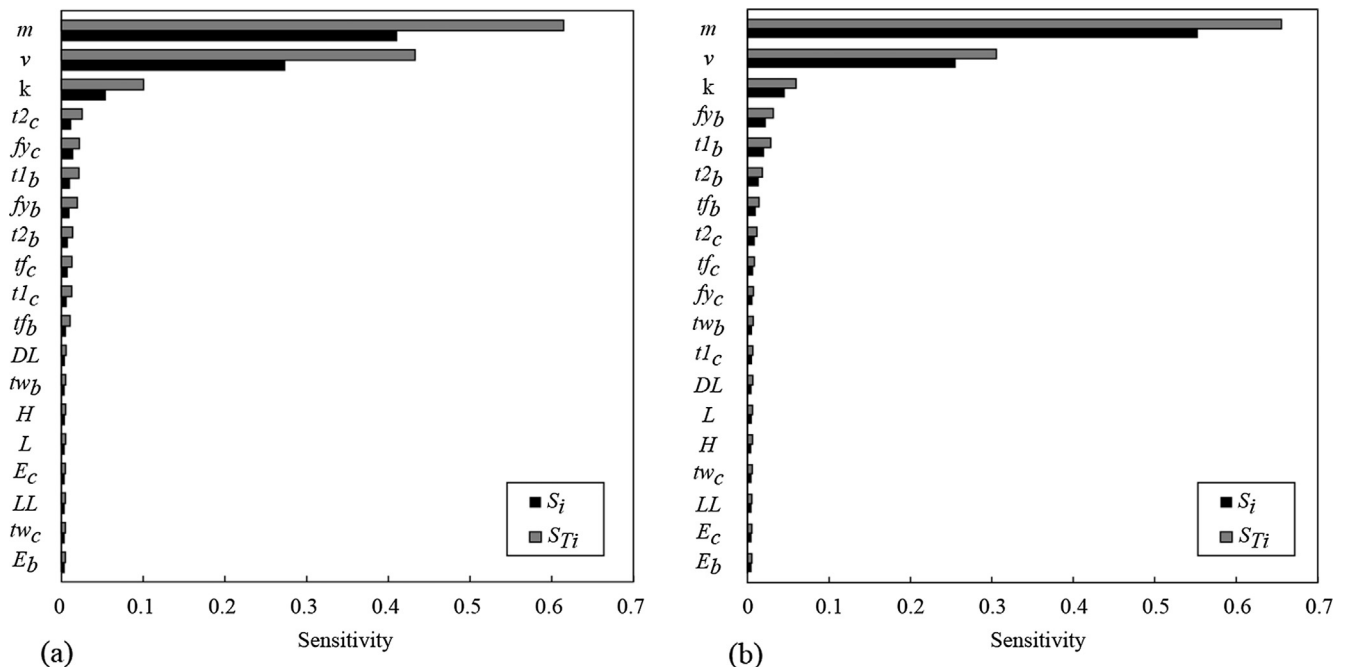


Fig. 12. First-order sensitivity indices and total effects.

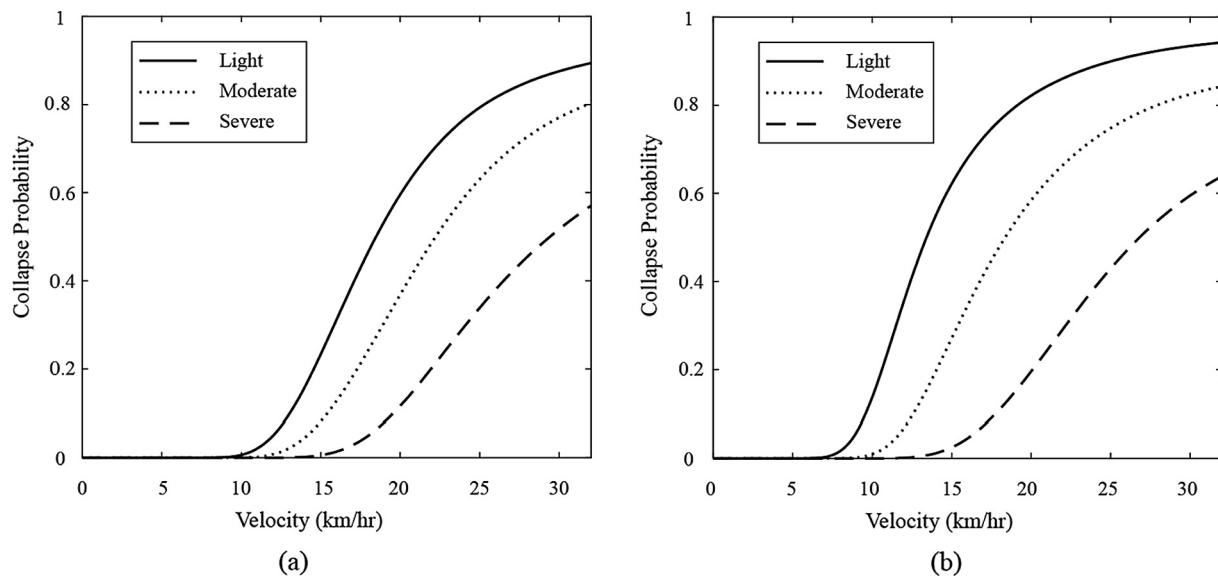


Fig. 13. Fragility curves for vehicle collision scenarios: (a) strong axis direction; (b) weak axis direction.

obtained using reliability analysis up to the velocity of 32 km/h for which the ANNs are trained properly. The range of velocity is divided into steps of 0.1 km/h and for each velocity 1×10^6 samples are used to carry out MCS.

The fragility curves for the two collision scenarios are shown in Fig. 13. It is seen that the structure is more vulnerable to collision in the weak axis direction and its fragility curves are bended slightly leftward. The median collapse velocities related to the light, moderate, and severe damage states are respectively 18.4 km/h, 22.2 km/h, and 29.4 km/h for the strong axis direction scenario and 13.4 km/h, 18.4 km/h, and 26.8 km/h for the weak axis direction scenario. Finally it should be noted that, as the ANNs are universal estimators, obtaining the fragility curves considering other parameters as the intensity measure is straightforward which is another advantage of neurocomputing.

8. Conclusions

In the present research, a new framework including both verified analytical and surrogate models was established to provide a basis for probabilistic collapse assessment of structures under extreme actions. The efficient ASI-Gauss technique was verified by experimental data and implemented in conjunction with a core neural network in the application by *MATLAB* programming. The developed method enables parametric structural modeling using *ASIFEM* to train the core ANN and conduct further probabilistic collapse assessment. To show the applicability of the established method, vulnerability of a steel moment frame structure under code-stipulated vehicle impact loads was investigated. The accuracy of the analysis model and the ANNs were validated first and then reliability assessment, sensitivity tests, and fragility analysis are conducted.

Based on analysis results, it was concluded that the established framework is suitable for collapse assessment under extreme loads and actions in which numerous probabilistic analyses are to be conducted. However, more attention must be paid to training ANNs for problems with highly nonlinear and non-monotonic responses. The results from the reliability analysis of the case study structure showed that the structure was highly vulnerable to vehicle impact loads on the corner column. The results from both sensitivity tests showed that vehicle parameters in the loading formula are the most influential factors in the output uncertainty. The overall collapse behavior of the structure was evaluated using fragility analysis, which showed that the probabilities of reaching the three different damage states are larger for impact loads

along the weak axis.

The analysis results showed that the computational efficiency for probabilistic collapse assessment of framed structures was improved in terms of realization and metamodeling using an efficient analytical model and artificial neural networks, respectively. However efficient models for more complicated structures or approximation of total collapse behavior of a whole structure using deep learning methods are still matters of debate. Moreover, fracture and contact between elements are not considered in this study which could give rise to extremely high nonlinearity and further inaccuracy in the metamodels. Thorough study is still required to cover the aforementioned limitations, which is beyond the scope of this research.

Acknowledgments

This research is supported by Basic Science Research Program through the National Research Foundation of Korea (NRF) funded by the Ministry of Education (NRF-2016R1D1A1B03932880).

References

- [1] Brunesi E, Nascimbene R, Parisi F, Augenti N. Progressive collapse fragility of reinforced concrete framed structures through incremental dynamic analysis. *Eng Struct* 2015;104:65–79. <http://dx.doi.org/10.1016/J.ENGSTRUCT.2015.09.024>.
- [2] Li Y, Lu X, Guan H, Ren P, Qian L. Probability-based progressive collapse-resistant assessment for reinforced concrete frame structures. *Adv Struct Eng* 2016;19:1723–35. <http://dx.doi.org/10.1177/1369433216649385>.
- [3] Yu XH, Lu DG, Qian K, Li B. Uncertainty and sensitivity analysis of reinforced concrete frame structures subjected to column loss. *J Perform Constr Facil* 2017;31:4016069. [http://dx.doi.org/10.1061/\(ASCE\)CF.1943-5509.0000930](http://dx.doi.org/10.1061/(ASCE)CF.1943-5509.0000930).
- [4] Wang Z, Pedroni N, Zentner I, Zio E. Seismic fragility analysis with artificial neural networks: application to nuclear power plant equipment. *Eng Struct* 2018;162:213–25. <http://dx.doi.org/10.1016/J.ENGSTRUCT.2018.02.024>.
- [5] Pu Y, Mesbahi E. Application of artificial neural networks to evaluation of ultimate strength of steel panels. *Eng Struct* 2006;28:1190–6. <http://dx.doi.org/10.1016/J.ENGSTRUCT.2005.12.009>.
- [6] Tsompanakis Y, Lagaros ND, Stavroulakis GE. Soft computing techniques in parameter identification and probabilistic seismic analysis of structures. *Adv Eng Softw* 2008;39:612–24. <http://dx.doi.org/10.1016/J.ADVENGSOFT.2007.06.004>.
- [7] Lagaros ND, Tsompanakis Y, Psaropoulos PN, Georgopoulos EC. Computationally efficient seismic fragility analysis of geostructures. *Comput Struct* 2009;87:1195–203. <http://dx.doi.org/10.1016/J.COMPSTRUC.2008.12.001>.
- [8] Chojaczyk AA, Teixeira AP, Neves LC, Cardoso JB, Soares CG. Review and application of Artificial Neural Networks models in reliability analysis of steel structures. *Struct Saf* 2015;52:78–89. <http://dx.doi.org/10.1016/J.STRUSAFE.2014.09.002>.
- [9] Möller B, Liebscher M, Schweizerhof K, Mattern S, Blankenhorn G. Structural collapse simulation under consideration of uncertainty – improvement of numerical efficiency. *Comput Struct* 2008;86:1875–84. <http://dx.doi.org/10.1016/J.COMPSTRUC.2008.04.011>.

- [10] de Lautour OR, Omenzetter P. Prediction of seismic-induced structural damage using artificial neural networks. *Eng Struct* 2009;31:600–6. <http://dx.doi.org/10.1016/J.ENGSTRUCT.2008.11.010>.
- [11] Giovanis DG, Papadopoulos V. Spectral representation-based neural network assisted stochastic structural mechanics. *Eng Struct* 2015;84:382–94. <http://dx.doi.org/10.1016/J.ENGSTRUCT.2014.11.044>.
- [12] Bojórquez J, Ruiz SE, Ellingwood B, Reyes-Salazar A, Bojórquez E. Reliability-based optimal load factors for seismic design of buildings. *Eng Struct* 2017;151:527–39. <http://dx.doi.org/10.1016/J.ENGSTRUCT.2017.08.046>.
- [13] Mitropoulou CC, Papadrakakis M. Developing fragility curves based on neural network IDA predictions. *Eng Struct* 2011;33:3409–21. <http://dx.doi.org/10.1016/J.ENGSTRUCT.2011.07.005>.
- [14] DoD (Department of Defense). Unified Facilities Criteria (UFC): design of buildings to resist progressive collapse. Washington, DC; 2005.
- [15] GSA (General Service Administration). Progressive collapse analysis and design guidelines for new federal office buildings and major modernization projects. Washington, DC; 2003.
- [16] Kim T, Kim J, Park J. Investigation of progressive collapse-resisting capability of steel moment frames using push-down analysis. *J Perform Constr Facil* 2009;23:327–35. [http://dx.doi.org/10.1061/\(ASCE\)0887-3828\(2009\)23:5\(327\)](http://dx.doi.org/10.1061/(ASCE)0887-3828(2009)23:5(327)).
- [17] Fu F. Progressive collapse analysis of high-rise building with 3-D finite element modeling method. *J Constr Steel Res* 2009;65:1269–78. <http://dx.doi.org/10.1016/J.JCSR.2009.02.001>.
- [18] Kim J, Lee S, Choi H. Progressive collapse resisting capacity of moment frames with viscous dampers. *Struct Des Tall Spec Build* 2013;22:399–414. <http://dx.doi.org/10.1002/tal.692>.
- [19] Li H, El-Tawil S. Three-dimensional effects and collapse resistance mechanisms in steel frame buildings. *J Struct Eng* 2014;140:A4014017. [http://dx.doi.org/10.1061/\(ASCE\)ST.1943-541X.0000839](http://dx.doi.org/10.1061/(ASCE)ST.1943-541X.0000839).
- [20] Shayanfar MA, Javidan MM. Progressive collapse-resisting mechanisms and robustness of RC frame-shear wall structures. *J Perform Constr Facil* 2017;31:4017045. [http://dx.doi.org/10.1061/\(ASCE\)CF.1943-5509.0001012](http://dx.doi.org/10.1061/(ASCE)CF.1943-5509.0001012).
- [21] Kang H, Kim J. Progressive collapse of steel moment frames subjected to vehicle impact. *J Perform Constr Facil* 2015;29:4014172. [http://dx.doi.org/10.1061/\(ASCE\)CF.1943-5509.0000665](http://dx.doi.org/10.1061/(ASCE)CF.1943-5509.0000665).
- [22] Fu F. Dynamic response and robustness of tall buildings under blast loading. *J Constr Steel Res* 2013;80:299–307. <http://dx.doi.org/10.1016/J.JCSR.2012.10.001>.
- [23] MATLAB; 2016.
- [24] El-Tawil S, Severino E, Fonseca P. Vehicle collision with bridge piers. *J Bridg Eng* 2005;10:345–53. [http://dx.doi.org/10.1061/\(ASCE\)1084-0702\(2005\)10:3\(345\)](http://dx.doi.org/10.1061/(ASCE)1084-0702(2005)10:3(345)).
- [25] Sharma H, Gardoni P, Hurlbeaus S. Probabilistic demand model and performance-based fragility estimates for RC column subject to vehicle collision. *Eng Struct* 2014;74:86–95. <http://dx.doi.org/10.1016/J.ENGSTRUCT.2014.05.017>.
- [26] Sharma H, Gardoni P, Hurlbeaus S. Performance-based probabilistic capacity models and fragility estimates for RC columns subject to vehicle collision. *Comput Civ Infrastruct Eng* 2015;30:555–69. <http://dx.doi.org/10.1111/mice.12135>.
- [27] Kang H, Kim J. Response of a steel column-footing connection subjected to vehicle impact. *Struct Eng Mech* 2017;63:125–36. <http://dx.doi.org/10.12989/sem.2017.63.1.125>.
- [28] CEN (European Committee for Standardization). Eurocode 1: actions on structures, part 1–7: general actions – accidental actions. Brussels; 2006.
- [29] ASIFEM; 2007. <http://www.kz.tsukuba.ac.jp/~isobe/asifem_e.html>.
- [30] Lynn KM, Isobe D. Structural collapse analysis of framed structures under impact loads using ASI-Gauss finite element method. *Int J Impact Eng* 2007;34:1500–16. <http://dx.doi.org/10.1016/J.IJIMPENG.2006.10.011>.
- [31] Isobe D, Thanh LTT, Sasaki Z. Numerical simulations on the collapse behaviors of high-rise towers. *Int J Prot Struct* 2012;3:1–19. <http://dx.doi.org/10.1260/2041-4196.3.1.1>.
- [32] Isobe D, Han WS, Miyamura T. Verification and validation of a seismic response analysis code for framed structures using the ASI-Gauss technique. *Earthq Eng Struct Dyn* 2013;42:1767–84. <http://dx.doi.org/10.1002/eqe.2297>.
- [33] Isobe D. An analysis code and a planning tool based on a key element index for controlled explosive demolition. *Int J High-Rise Build* 2014;3:243–54.
- [34] Sadek F, Main JA, Lew HS, Robert SD, Chiarito VP, El-Tawil S. An experimental and computational study of steel moment connections under a column removal scenario. Gaithersburg, MD: NIST; 2010.
- [35] Elhewy AH, Mesbahi E, Pu Y. Reliability analysis of structures using neural network method. *Probabilistic Eng Mech* 2006;21:44–53. <http://dx.doi.org/10.1016/J.PROBENGMECH.2005.07.002>.
- [36] Cardoso JB, de Almeida JR, Dias JM, Coelho PG. Structural reliability analysis using Monte Carlo simulation and neural networks. *Adv Eng Softw* 2008;39:505–13. <http://dx.doi.org/10.1016/J.ADVENGSOFT.2007.03.015>.
- [37] Waszczyszyn Z. Neural networks in the analysis and design of structures. Springer 1999. <http://dx.doi.org/10.1007/978-3-7091-2484-0>.
- [38] Ayyub BM, Lai K-L. Structural reliability assessment using Latin hypercube sampling. In: 5th int conf struct saf reliab., Reston, VA: ASCE; 1990. p. 1177–84.
- [39] Viana FAC. A tutorial on Latin hypercube design of experiments. *Qual Reliab Eng Int* 2016;32:1975–85. <http://dx.doi.org/10.1002/qre.1924>.
- [40] Latin hypercube sample – MATLAB lhsdesign; n.d. <<https://www.mathworks.com/help/stats/lhsdesign.html>> [accessed June 3, 2018].
- [41] Ellingwood B, Galambos TV, MacGregor JG, Cornell CA. Development of a probability based load criterion for American National Standard A58 – building code requirement for minimum design loads in buildings and other structures. Washington, DC: National Bureau of Standards, Dept. of Commerce; 1980.
- [42] JCSS (Joint Committee on Structural Safety). Probabilistic model code; 2001.
- [43] CEN (European Committee for Standardization). EN 10034:1993. Structural steel I and H sections – tolerances on shape and dimensions. Brussels; 1993.
- [44] Hallquist J. LS-Dyna keyword user's manual. CA: Livermore; 2007.
- [45] Conrath EJ, Krauthammer T, Marchand KA, Mlakar PF. Structural design for physical security – state of the practice. New York: ASCE; 1999.
- [46] Shooman ML. Probabilistic reliability: an engineering approach. New York: McGraw-Hill; 1986.
- [47] CEN (European Committee for Standardization). Eurocode: basis of structural design. Brussels; 2002.
- [48] Kim J, Park JH, Lee TH. Sensitivity analysis of steel buildings subjected to column loss. *Eng Struct* 2011;33:421–32. <http://dx.doi.org/10.1016/J.ENGSTRUCT.2010.10.025>.
- [49] Saltelli A, Ratto M, Andres T, Campolongo F, Cariboni J, Gatelli D, et al. Global sensitivity analysis: the primer. Chichester, U.K.: John Wiley & Sons; 2008.
- [50] Sobol IM. Sensitivity estimates for nonlinear mathematical models. *Mat Model* 1990;2:112–8.
- [51] Sobol IM. Global sensitivity indices for nonlinear mathematical models and their Monte Carlo estimates. *Math Comput Simul* 2001;55:271–80. [http://dx.doi.org/10.1016/S0378-4754\(00\)00270-6](http://dx.doi.org/10.1016/S0378-4754(00)00270-6).
- [52] Homma T, Saltelli A. Importance measures in global sensitivity analysis of nonlinear models. *Reliab Eng Syst Saf* 1996;52:1–17. [http://dx.doi.org/10.1016/0951-8320\(96\)00002-6](http://dx.doi.org/10.1016/0951-8320(96)00002-6).
- [53] Kala Z. Sensitivity assessment of steel members under compression. *Eng Struct* 2009;31:1344–8. <http://dx.doi.org/10.1016/J.ENGSTRUCT.2008.04.001>.
- [54] Kala Z. Sensitivity analysis of steel plane frames with initial imperfections. *Eng Struct* 2011;33:2342–9. <http://dx.doi.org/10.1016/J.ENGSTRUCT.2011.04.007>.
- [55] Kala Z. Global sensitivity analysis in stability problems of steel frame structures. *J Civ Eng Manage* 2016;22:417–24. <http://dx.doi.org/10.3846/13923730.2015.1073618>.
- [56] Arwade SR, Moradi M, Louhghalam A. Variance decomposition and global sensitivity for structural systems. *Eng Struct* 2010;32:1–10. <http://dx.doi.org/10.1016/J.ENGSTRUCT.2009.08.011>.
- [57] Saltelli A, Tarantola S, Campolongo F, Ratto M. Sensitivity analysis in practice: a guide to assessing scientific models. Chichester, U.K.: John Wiley & Sons; 2004.
- [58] Park JH, Kim J. Fragility analysis of steel moment frames with various seismic connections subjected to sudden loss of a column. *Eng Struct* 2010;32:1547–55. <http://dx.doi.org/10.1016/J.ENGSTRUCT.2010.02.003>.